Volume 1 | Number 1 | Jan 2013 | Pages 1–100

Metallomics

Integrated biometal science
www.rsc.org/metallomics

ROYAL SOCIETY OF CHEMISTRY

ROYAL SOCIETY OF CHEMISTRY

www.rsc.org/metallomics

Inhibition of human DNA topoisomerase IB by nonmutagenic ruthenium(II)-based compounds with antitumoral activity

Mariana S. de Camargo[a*], Monize M. da Silva[a], Rodrigo S. Correa[b], Sara D. Vieira[c], Silvia Castelli[c], Ilda D'Anessa[c], Rone De Grandis[d], Eliana Varanda[d], Victor M. Deflon[e], Alessandro Desideri[c*], Alzir A. Batista[a]

[a]Departamento de Química, Universidade Federal de São Carlos, CP 676, CEP 13565-905, São Carlos, SP, Brazil.

[b]Departamento de Química, ICEB, Universidade Federal de Ouro Preto, CEP 35400-000, Ouro Preto, MG, Brazil.

[c]Dipartimento di Biologia, Università Tor Vergata di Roma, 00133 Rome, Italy.

[d]Departamento de Ciências Biológicas, Faculdade de Ciências Farmacêuticas, UNESP, CEP 14800-900, Araraquara, SP, Brazil**.**

[e]Instituto de Química de São Carlos, Universidade de São Paulo, CP 780, CEP 13560-970, São Carlos, SP, Brazil.

Abstract

Herein we synthesized two new ruthenium (II) compounds [Ru(pySH)(bipy)(dppb)]PF$_6$ **(1)** and [Ru(HSpym)(bipy)(dppb)]PF$_6$ **(2)** that are analogs with a antitumor agent recently described, [Ru(SpymMe$_2$)(bipy)(dppb)]PF$_6$ **(3)** by [(Spy) = 2-Mercaptopyridine anion; (Spym) = 2-mercaptopyrimidine anion and (SpymMe$_2$) = 4,6-dimethyl-2-mercaptopyrimidine anion. *In vitro* cell culture experiments revealed a significant anti-proliferative activity of **1-3** against HepG2 and MDA-MB-231 tumor cells, higher than the standard anti-cancer drugs doxorubicin and cisplatin. No mutagenicity is detected when compounds are evaluated by Cytokinesis-blocked micronucleus cytome and Ames test in presence and absence of S9 metabolic activation from rat liver. Interaction studies shows that compounds **1-3** can bind to DNA through electrostatic interaction and with albumin through hydrophobic interaction. The three compounds are able to inhibit the DNA supercoiled relaxation mediated by the human topoisomerase IB (Top 1). Compound **3** is the most efficient Top 1 inhibitor and the inhibitory effect is enhanced upon pre-incubation with enzyme. Analysis of the different steps of Top 1 catalytic cycle indicates that **3** inhibits the cleavage reaction impeding the binding of the enzyme to DNA and slow down the religation reaction. Molecular docking show that **3** preferentially binds close to the residues of the active site when Top1 is free and lays on the DNA groove downstream of the cleavage site in Top 1-DNA complex. Thus, **3** can be considered in further studies for a possible use as anticancer agent.

1. Introduction

Despite the development of novel drugs, cancer remains one of the major causes of death in the world[1]. Chemotherapy is the most exploited cancer therapy and metal compounds can be useful drugs for such purpose[2]. Cisplatin is a solid example of an active metallodrug used for treating cancer, but because of side effects, there is an increasing need of development of new anticancer drugs. In this direction ruthenium based compounds have been proposed as potential antitumor agents, having an antimetastatic behavior and showing systemic toxicity lower than platinum compounds[3]. Some of these compounds preferentially bind to proteins, but also to DNA nucleobases modifying their conformation inducing DNA unwinding[4-6].

Most antitumor agents are designed to act in cell proliferation[7] inhibiting DNA synthesis by two mechanisms that are generally associated: the drug either interacts with DNA by intercalation and stops its replication[8], or it interferes directly with molecules required for DNA polymerization and/or initiation of its replication[9, 10]. DNA intercalating drugs can induce mutations that can lead to aberrations in normal cells and conversion of non-carcinogenic cells into carcinogenic cells[11]. Chemotherapeutic drugs must then be tested not only for their anticancer or antitumor activity, but also for their potential mutagenicity[12].

Ruthenium compounds present rich photochemical properties and have received attention as possible topoisomerase inhibitors[13]. DNA topoisomerases are involved in many vital cellular processes that influence DNA replication, transcription, recombination, integration, and chromosomal segregation, and are important targets to be considered in the development of potential cytotoxic agents[14,15, 16].

All the topoisomerases act introducing transient strand breaks in a DNA double strand molecule. In particular, human topoisomerase IB forms a covalent bond with the

3´-phosphate end of the cleaved strand[17]. During this state, the broken strand can rotate around the uncleaved strand leading to DNA relaxation[18-20]. To restore the correct DNA double strand structure, topoisomerase I catalyzes the religation of the 5´-hydroxyl termini[15].

Topoisomerase IB (Top1) is the target of several drugs that, depending on their action mechanism, are classified as poisoning or as catalytic inhibitors[21, 22]. Poison inhibitors include clinically used drugs, such as the derivatives of the natural compound camptothecin, as well as compounds in clinical development such as the indenoisoquinolines[23]. Both reversibly bind the covalent Top1–DNA complex slowing down the religation of the cleaved DNA strand, inducing cell death[24, 25]. Two main analogs of camptothecin, topotecan and irinotecan, which are DNA topoisomerase I poisons, are successfully used to treat several human cancers and have been approved by the US Food and Drug Administration for clinical purposes[9, 26]. Catalytic inhibitors are compounds that prevent topoisomerase I binding to DNA or inhibit the cleavage reaction of the enzyme and consequently inhibit the DNA relaxation[26, 27]. Recently, some compounds have been found to be able to inhibit both cleavage and religation[28, 29].

As part of our ongoing effort to develop new ruthenium compounds as promising antitumor agents, we present the synthesis and characterization of two new ruthenium compounds $[Ru(pySH)(bipy)(dppb)]PF_6$ (**1**) and $[Ru(HSpym)(bipy)(dppb)]PF_6$ (**2**), and compared their antitumoral activity with the analog $[Ru(SpymMe_2)(bipy)(dppb)]PF_6$ (**3**), a potent agent against breast tumor cell[30] in order to understand their biological activities. Compounds **1-3** were evaluated for their cytotoxicity, *in vitro,* against HepG2, MDA-MB-231 and CHO cells. Also their ability to interact with DNA and albumin, their mutagenicity and their inhibitory activity against Top 1 were carried out.

4

2. Experimental

2.1. General

Reactions and chemicals were handled under argon atmosphere. Solvents were purified by standard methods. All chemicals used were of reagent grade or comparable purity. The $RuCl_3.3H_2O$ was purchased from Aldrich. The ligands 1,4-bis (diphenylphosphino) butane (dppb), 2,2'-bipyridine (bipy), 2-Mercaptopyridine (HSpy), 2-mercaptopyrimidine (HSpym) and 4,6-dimethyl-2-mercaptopyrimidine (HSpymMe$_2$) were used as received from Aldrich. The *cis*-[RuCl$_2$(dppb)(bipy)] compound was prepared according to published procedures[31].

The infrared spectra used CsI pellets in as FTIR Bomem-Michelson 102 spectrometer in the 4000-200 cm^{-1}region. Cyclic voltammetry experiments were performed in an electrochemical analyzer BAS, model 100B and were carried out at room temperature. Typical conditions were: Typical conditions were: CH_2Cl_2 containing 0.10 mol L^{-1} of Bu$_4$NClO$_4$ (TBAP) as a support electrolyte, using a electrochemical cell, a three electrode system was used, which was glassy carbon as a working electrode (CG), Ag/AgCl as a reference electrode and platinum plate as a auxiliary electrode.

The microanalyses were performed in the Microanalytical Laboratory at the Universidade Federal de São Carlos, São Carlos (SP)-Brazil, with an EA 1108 CHNS microanalyser (Fisions Instruments). Conductivity values were obtained at room temperature using 10^{-3} M solutions of the compounds in CH_2Cl_2 by a Meter Lab CDM2300 instrument. ^1H and $^{31}P\{^1H\}$ were recorded on a Bruker DRX 400 MHz using chemical shifts, which are reported in relation to H_3PO_4, 85%.

X-ray crystallography, orange crystals were grown by slow evaporation of a dichloromethane/methanol solution. The data collections for the X-ray structure

determinations were performed using Mo-Kαradiation (λ= 71.073 pm) on a BRUKER APEX II Duo diffractometer. Standard procedures were applied for data reduction and absorption correction. The structures were solved with SHELXS97 using direct methods[32] and all non-hydrogen atoms were refined with anisotropic displacement parameters with SHELXL97[33].The hydrogen atoms were calculated at idealized positions using the riding model option of SHELXL97[33].

2.2.Synthesis

The compound **3** was previously described in the literature[30] and **1** and **2** were synthesized based on the same procedure[30]. The compounds **1** and **2** w were prepared by reacting the *cis*-[RuCl$_2$(dppb)(bipy)] precursor (0.132 mmol,100.0 mg) with the ligands HSpy and HSpym (0.15 mmol, 17.0 mg)and 0.132 mmol (24.3 mg) of KPF$_6$ in methanol (50 mL) under Ar atmosphere for 24 hours. The final orange solution was concentrated to ca. 2 mL and diethyl ether was added, to obtain orange precipitate. The solid was filtered off, well rinsed with water (5 x 5 mL) and diethyl ether (3 x 5 mL) and dried *in vacuo*.

Compound **1**: Yield of 114 mg (92%). Anal.Calcd for C$_{44}$H$_{40}$F$_6$N$_3$P$_3$RuS: exptl (calc) C, 55.00 (55.01); H, 4.29 (4.29); N, 4.50 (4.48); S, 3.42 (3.42). ^{31}P{^{1}H} NMR: δ(ppm) 42.00 (d); 41.24 (d), ^{2}J$_{p-p}$ = 35.64 Hz^{1}H NMR (400 MHz, CDCl$_3$, 298 K): δ(ppm) 9.14 (d, 1H,^{3}J = 5.4 Hz); 8.93 (d, 1H, ^{3}J = 4.0 Hz); 8.39 (d, 1H, ^{3}J = 7.8 Hz); 8.21 (d, 1H, ^{3}J = 7.6 Hz); 8.11 (t, 1H, ^{3}J = 8.0 Hz); 7.79 (t, 1H, ^{3}J = 7.6 Hz); 7.57 (t, 1H, ^{3}J = 8.0 Hz); 7.44 (t, 1H, ^{3}J = 7.2 Hz) (aromatic hydrogens for bipy); 7.34–6.56 (overlapped signals, 20H aromatic hydrogens for dppb); 4.0–1.0 (8H, CH$_2$ of dppb); 6.61(t, 1H, ^{3}J = 8.0 Hzof Spym); 6.49 (d, 1H, ^{3}J = 8.0 Hz of Spym); 5.95 (t, 1H, ^{3}J=8.0 of Spym).;5.75 (d, 1H, ^{3}J=4.0 of Spym). Molar conductance (μS/cm, CH$_2$Cl$_2$) 42.5.IR (cm^{-1}): (νC-H) 3075, 3015, 2955, 2915; (νCH2) 2857; (νC=N) 1580, 1434; (ν-C=C(ring) + νC=C(dppb))

6

1482, 1310; (vC-S) 1159; (vC-P) 1094; ($v$ring) 1043, 997; (vP-F) 839; (γC=S) 768;

(γring) 696; (vP-F) 557; (vRu-P) 519, 507; (vRu-S) 458; (vRu-N) 419.

Compound **2**:Yield of 108 mg (87%). Anal.Calcd for $C_{42}H_{39}F_6N_4P_3RuS$: exptl (calc) C, 53.66 (53.67); H, 4.18 (4.18); N, 5.93 (5.96); S, 3.42 (3.41). $^{31}P\{^1H\}$ NMR: δ(ppm) 42.83 (d); 40.46 (d), $^2J_{p\text{-}p} = 36.45$ Hz. ^1H NMR (400 MHz, CDCl$_3$, 298 K): δ(ppm) 9.14 (d, 1H,$^3J = 5.6$ Hz); 8.71 (d, 1H, $^3J = 4.0$ Hz); 8.40 (d, 1H, $^3J = 7.6$ Hz); 8.23 (d, 1H, ^3J = 7.2 Hz); 8.13 (t, 1H, $^3J = 7.9$ Hz); 7.79 (t, 1H, $^3J = 7.4$ Hz); 7.58 (t, 1H, $^3J = 8.1$ Hz); 7.48 (t, 1H, $^3J = 7.4$ Hz) (aromatic hydrogens for bipy); 7.34–6.56 (overlapped signals, 20H aromatic hydrogens for dppb); 4.0–1.0 (8H, CH$_2$ of dppb);8.67 (d, 1H, $^3J = 4.8$ Hz of Spym); 8.61 (d, 1H, $^3J = 4.8$ Hz of Spym); 6.69 (t, 1H, ^3J=8.0 of Spym). Molar conductance (μS/cm, CH$_2$Cl$_2$) 41.4.IR (cm^{-1}): (vC-H) 3064, 3015, 2955, 2917; (vCH$_2$) 2862; (vC=N) 1541, 1432; (v-C=C(ring) + vC=C(dppb)) 1481, 1310; (vC-S) 1156; (vC-P) 1093; ($v$ring) 1051, 997; (vP-F) 842; (γC=S) 771; (γring) 696; (vP-F) 557; (vRu-P) 519, 508; (vRu-S) 494; (vRu-N) 422.

2.3.Cell culture and study of antiproliferative activity

The *in vitro* cytotoxic potency of compounds was evaluated by MTT assay against MDA-MB-231 (Human Breast Adenocarcinoma ATCC No. HTB-26), HepG2 (Human Hepatocellular Carcinoma purchased from the Rio de Janeiro Cell Bank, Brazil) and CHO (Chinese Hamster Ovary cells kindly provided by Dr. Catarina Satie Takahashi from the Faculdade de Medicina da Universidade de São Paulo-SP, Brazil). The three cell lines were grown in DMEM supplemented with 10% FCS (v/v), antibiotic–antimycotic Solution (1000 U of penicillin, 100 μg/mL of streptomycin sulfate and 0.25 μg/mL amphotericin B), and kanamycin sulfate (100 μg/mL). Cells were kept in a humidified atmosphere with 5% CO$_2$ at 37 °C. After reaching

7

confluence, the cells were removed from the flasks using ethylenediaminetetraacetic acid (EDTA) (10 mM) in phosphate buffered saline and were counted for the experiments.

To evaluate the cytotoxic activity of compounds, the cell viability was determined by the MTT test [3-(4,5-dimethylthiazol-2-yl)-2,5-diphenyltetrazolim bromide], a colorimetric assay determined by the mitochondrial-dependent reduction of the soluble yellow tetrazolium salt to blue formazan crystals [34]. The cells were seeded onto a 96-well plate (1×10^4 cells per well) in 200 μL of the appropriate complete medium 24 h prior to the beginning of the experiment. Stock solutions of the ruthenium compounds, doxorubicin and cisplatin were prepared in sterile DMSO (20 mM). The stock solution of the compounds and control drugs were diluted directly into the medium in order to achieve different final concentrations (0.01220 – 200 µM), with a final concentration of 1% DMSO. Twenty-four hours after the addition of **1-3** or the vehicle, MTT (0.5 mg mL^{-1}) was added and the cells were incubated for a period of 3 h. The optical density was measured after dissolving the blue formazan crystals into 200 μL of isopropanol, and the cell viability was determined by absorbance measurements at 540 nm[35, 36]. The amounts of surviving cells, compared to those of the untreated controls, were determined. The IC$_{50}$ values, defined as the drug concentration that inhibits cell growth by 50%, were estimated graphically using dose-response plots.

2.4. ct-DNA binding experiments

2.4.1. Compound-DNA interactions by UV-Visible

Calf thymus DNA solution (ct-DNA, purchased from Sigma-Aldrich) was prepared dissolving the DNA in a Tris-HCl buffer (5 mMTris-HCl, pH 7.2). The ration of the absorbance at 260 and 280 nm (A260/A280) of the ctDNA solution was between 1.8-2, indicating that the solution is protein-free. The concentration of ct-DNA was

measured from its absorption intensity at 260 nm using the molar absorption coefficient value of 6600 M^{-1} cm^{-1} [37]. The solution of ruthenium compounds **1-3** used in the experiments was prepared in a Tris-HCl buffer containing 5 % DMSO. In the titration experiments, different concentrations of the ctDNA were used while the ruthenium complex was at 50μM. Sample correction was made for the absorbance of ctDNA and the spectra were recorded after solution equilibration for 2 min. The intrinsic equilibrium binding constant (Kb) of the compounds to ct DNA was obtained by monitoring changes in the absorption intensity with increasing concentration of ctDNA, and was analyzed by regression analysis.

2.4.2. Compound-DNA interactions by square-wave voltammetry (SWV)

The compound-DNA interactions were performed by square-wave voltammetry (SWV). In the SWV, a three electrode system was used, which was glassy carbon as a working electrode (CG), Ag/AgCl as a reference electrode and platinum plate as acounter electrode. The interaction studies were carried out in a Tris-HCl buffer (pH 7.4) 30% DMSO. The titration was performed by adding 50 µL aliquots of the DNA (4.2 mM) electrochemical cell, containing 2 mL of the compound solution 1x10^{-3}M.

2.4.3. Compound-DNA interactions by viscosity

Viscosity measurements were carried out according to Carter et. al. (1989)[38] using an Ostwald viscometer immersed in a water bath maintained at 25 °C. The DNA concentration in the buffer Tris–HCl was kept constant in all samples, while the compound (**1-3**) concentration was increased. The flow time was measured at least 5 times and the mean value was calculated. Data are presented as $(\eta/\eta_0)^{1/3}$ versus the [compound]/[DNA] ratio, where η and η_0 are the specific viscosities of DNA in the presence and absence of the compound, respectively. The values of η and η_0 were

calculated using the expression $(t - t_b)/t_b$, where t is the observed flow time and t_b is the flow time of buffer alone[39,40,41]

2.5.BSA (bovine serum albumin) interactions study

The protein interaction was examined in 96-well plates used for fluorescence assays. BSA (2.5 µM) was prepared by dissolving the protein in buffer (4.5 mM Tris-HCl, 0.5 mM NaOH, 50 mM NaCl) at pH 7.4. For fluorescence measurements, the BSA concentration in the buffer Tris–HCl was kept constant in all samples, while the compound concentration was increased from 3.13 to 200 µM in DMSO, and quenching of the emission intensity of the BSA's tryptophan residues at 344 nm (excitation wavelength 295 nm) was monitored at different temperatures (295, 300, 305 and 310 K). Measurements of interaction with BSA were taken using a SpectraMax M3 fluorometer.

The inner filter effect on the intensity of fluorescence of BSA and compounds was previously corrected according to the equation[42] :

$$F_{corr} = F_{obs} \, e^{\frac{(Aem)+Aex)}{2}}$$

Where F_{corr} and A_{obs} are the corrected and observed fluorescence intensities, respectively. A_{ex} and A_{em} are the absorbance values of the drugs at the excitation and emission wavelengths, respectively.

2.6.Mutagenicity assays

2.6.1.   Ames test

Mutagenic activity was evaluated by the Salmonella/microsome assay, using the *Salmonella typhimurium* tester strains TA98, TA100, TA97a and TA102, kindly provided by Dr. B.N. Ames (Berkeley, CA, USA), with (+ S9) and without (− S9) metabolization, by the pre-incubation method [43].

To determine the mutagenic activity, five different concentrations of the compounds (1.56 – 75.0 μg⁄ plate), diluted in DMSO, were assayed. The concentrations of compounds were selected on the basis of a preliminary toxicity test. In all subsequent assays, the upper limit of the dose range tested was either the highest non-toxic dose or the lowest toxic dose determined in this preliminary assay.

All experiments were analyzed in triplicate. The results were analyzed using the statistical software package Salanal 1.0 (U.S. Environmental Protection Agency, Monitoring Systems Laboratory, Las Vegas, NV, from Research Triangle Institute, RTP,NC, USA), adopting the Bernstein et al.[44] model. The data (revertants/ plate) were assessed by analysis of variance (ANOVA), followed by linear regression. The mutagenic index (MI) was also calculated for each concentration tested, which was the average number of revertants per plate with the test compound divided by the average number of revertants per plate with the negative (solvent) control. A test solution was considered mutagenic when a dose–response relationship was detected and a two-fold increase in the number of mutants (MI $\geq$ 2) was observed for at least one concentration[45]. The standard mutagens used as positive controls in experiments without S9 mix were 4 -nitro-o-phenylenediamine (NOPD) (10 μg/ plate) for TA98 and TA97a, sodium azide (SA) (1.25 μg/ plate) for TA100 and mitomycin (MMC) (0.5 μg/ plate) for TA102. In experiments with S9 activation, 2-anthramine (2-AA) (1.25 μg /plate) was used with TA98, TA97a and TA100 and 2-aminofluorene (2-AF) (10 μg/ plate) with TA102. DMSO (50 μL/ plate) served as the negative (solvent) control.

11

2.6.2. Cytokinesis-blocked micronucleus cytome assay(CBMN-cyt)

The mutagenicity was evaluated as described by Fenech et al. (2007)[46] with modifications. Three different concentrations (IC$_{50}$ and two lower) were used for CBMN-cyt analysis. For **1** 2.07, 0.78, 0.48 µM, for **2** 3.23 0.78, 0.48 µM and for **3** 2.26, 0.78, 0.48 µM. A total of 5×10^5 HepG2 cultures as previously described were incubated in 25 cm^2 culture flasks for 24 h and then treated with the three different concentrations of the ruthenium compounds or 0.03 µg/mL doxorubicin. After 20 h of treatment (44 h after the initiation of the culture), the cells were washed with PBS, the culture media was changed, and cytochalasin B (final concentration of 3.0 µg/mL) was added. The cells were then incubated for an additional 28 h, harvested, treated with cold hypotonic solution (0.01% sodium citrate) and fixed with formaldehyde and methanol–acetic acid (3:1). The slides were stained immediately before analysis using 40 µg/mL acridine orange, and the binucleated cells with 1–4 micronuclei (MNi) were scored at 1000× magnification. Additionally, the frequency of nucleoplasmic bridges (NPBs) and nuclear buds (NBUDs) were evaluated using the criteria of Fenech et al. (2007). The Nuclear Division Index (NDI) was also calculated to evaluate the altered mitotic activity and/or cytostatic effects according to the following formula[47]: NDI = $(M_1 + 2M_2 + 3M_3 + 4M_4)/N$, where M_1, M_2, M_3 and M_4 are the number of cells with one, two, three and four nuclei and N is the number of cells assayed.

A total of 500 cells per treatment were analyzed for the NDI calculation and 1000 binucleated cells for the MNi, NPBs and NBUDs frequencies. A total of three independent experiments were performed.

2.7. Topoisomerase IB assays

2.7.1. Purification of human topoisomerase IB

The human topoisomerase IB was expressed under the galactose inducible promoter in a multi-copy plasmid, YCpGAL1-e-wild type and YCpGAL1-e-Y723F, used for the transformation of EKY3 cells, as described previously [48].

The epitope-tagged constructs contain the N-terminal sequence FLAG: DYKDDDY (indicating with ''e''), recognized by the M2 monoclonal antibody. Purification was carried out using an ANTI-FLAG M2 Affinity Gel (Sigma) column. The FLAG-fusion topoisomerase IB was eluted by competition with five column volumes of a solution containing a 100 μg/mlFLAG peptide in 50 mMTris–HCl,150mM KCl, pH 7.4. Glycerol was added to each fraction and collected up to a final concentration of 40%. All the fractions were stored at -20 °C. Integrity of the protein was verified by the immunoblot assay. The purified protein was resolved on SDS-PAGE, transferred to nitrocellulose membrane and immunoblotted with a specific monoclonal antibody (Sigma-A9469). An immunoreactive band, corresponding to topoisomerase I, was detected with the BCIP/ NBT substrate (Sigma-B3804).

2.7.2. Topoisomerase IB activity *in vitro*: DNA relaxation assay

The activity of Top1 was assayed in 30 μL of reaction volume containing 0.5 μg of negatively supercoiled pBlue-Script KSII(+) and Reaction Buffer (20 mMTris–HCl, 0.1 mM EDTA, 10 mM $MgCl_2$, 50 μg/mL acetylated BSA and 150 mMKCl, pH 7.5). The effects of the **1-3** on enzyme activity were measured by adding increasing concentrations of the compounds to a final concentration of 0.75 to 400 μM. Reactions were stopped with a final concentration of 0.5% SDS after each time point at 37 °C. The samples were electrophoresed in 1% agarose gel in 50 mMTris, 45 mM boric acid, 1 mM EDTA. The gel was stained with ethidium bromide (5 μg/mL), destained with water and photographed under UV illumination. Where indicated, the enzyme and

inhibitor were pre-incubated at 37 °C for 5 min, before adding the DNA substrate. Assays were performed at least three times, but only one representative gel is shown.

2.7.3. Cleavage kinetics

The oligonucleotide substrate CL14 (5'-GAAAAAAGACTTAG-3') radiolabelled with $[\gamma^{-32}P]$ ATP at its 5' end and the CP25 complementary strand (5'-TAAAAATTTTTCTAAGTCTTTTTTC-3'), phosphorylated at its 5' end with unlabeled ATP, were annealed at a 2-fold molar excess of CP25 over CL14, creating the so called ''suicide substrate'', which contains only a partial duplex. The suicide cleavage reactions were carried out incubating 20 nM of suicide substrate with the enzyme in a reaction buffer at 37 °C and in the presence of 50 µM of compound **3**. DMSO was added to no-drug control. Before adding the enzyme, a 5 µL sample of the reaction mixture was removed and used as control. At different time points, 5 µL aliquots were removed and the reactions stopped with 0.5% SDS. Afterwards, the ethanol precipitation samples were re-suspended in 6 µL of 1 mg ml^{-1} trypsin and incubated at 37 °C for 1 hour. Samples were analyzed using denaturing urea/poly acrylamide gel electrophoresis. Where indicated, 6.25 µM compound was pre-incubated with the enzyme for 5 min before DNA addition.

The experiment was replicated at least three times and a representative gel is shown.

2.7.4. Religation kinetics

A suicide CL14/CP25 substrate (20 nM), prepared as above, was incubated with topoisomerase IB enzyme for 30 min at 37 °C in reaction Buffer. A 5 µL aliquote of the reaction mixture was removed and used as the zero time point. Religation reactions were initiated by adding a 200-fold molar excess of R11 oligonucleotide (5'-AGAAAAATTTT-3') over the duplex CL14/CP25 in the presence or absence of 50 µM of **3**. At different times, 5 µL aliquots were removed and the reactions stopped with

0.5% SDS. After ethanol precipitation samples were re-suspended in 5 µL of 1 mg ml^{-1}

trypsin and incubated at 37 °C for 1 hour. Samples were analyzed by denaturing

urea/polyacrylamide gel electrophoresis. The experiment was replicated three times and

a representative gel is shown.

2.7.5. Electrophoretic mobility shift assay

The shift in DNA mobility due to topoisomerase binding was carried out using a 25 *mer*

fully duplex oligonucleotide CL25/CP25. The reaction was performed with the Y723F

topoisomerase IB mutant which is catalytically inactive, this enzyme is able to non-

covalently bind the DNA with the same affinity of the wild type[49].

The inactive enzyme was incubated under standard reaction conditions [20 mMTris–

HCl, pH 7.5, 0.1 mM Na$_2$EDTA, 10 mM MgCl$_2$, 50 µg ml^{-1} acetylated BSA and 150

µM KCl] in the presence of 1% (v/v) DMSO or 50 µM of compound **3** at 37°C.The

binding reaction was performed at 37 °C for 30 min. In a final volume of 30 µL, 5 µL of

dye was added to each sample [0.125% Bromophenol Blue and 40% (v/v) glycerol].

Samples were loaded onto 6% (v/v) native polyacrylamide gels and electrophoresed at

40 V in TBE buffer (12 mM Tris, 11.4 mM boric acid and 0.2 mM EDTA) at 4 °C for 4

hours. Products were visualized by PhosphorImager.

2.8.Molecular docking procedure

Docking was performed using the Autodock 4 program, with the AutodockTools suite

version 4 to prepare the ligand's and receptor's structures[50]. The Docking runs with the

free protein were carried out using the structure coming from the crystal structures

1A36[18]and 1EJ9[51], where missing residues were reconstructed with a procedure

previously described[52], after eliminating the DNA substrate. The docking with the

covalent complex was carried out using the three-dimensional co-ordinates from the

ternary complex crystal structure 1K4T [53], after eliminating TPT. The structure of **3** was

characterized by spectroscopic and electrochemical techniques and X-ray crystallography and elemental analysis[30]. For the docking experiment, 250 runs were performed, using the Lamarckian Genetic Algorithm[54]. The simulative box [38×48×38 Å] was built to contain the inner cavity of the protein involved in the interaction with the DNA and centred on its geometric centre. The analysis of the contacts between the ligand and the receptor in all the resulting structures was performed using an in-house modified version of the program g_mindistfrom the Gromacs 3.3.3 package[55], taking a threshold value of 3.5 Å. Clustering was carried out using the Autodock program based on an energetic score. The centroids of the clusters were then grouped into families based on their position.

Eletronic supplementary information

Supplementary crystallographic data for compounds $[Ru(pySH)(bipy)(dppb)]PF_6$ and $[Ru(HSpym)(bipy)(dppb)]PF_6$ (CCDC 1056229 and 1056230, respectively) can be obtained free of charge via http://www.cdc.cam.ac.uk/conts/retrieving.html, or from the Cambrigde Crystallographic Data Centre, 12 Union Road, Cambridge CB2 1 EZ, UK; fax: +44 1223 336 033; or e-mail: deposit@ccdc.com.ac.uk.

3. Results and discussion

3.1.Synthesis and characterization

The synthesis of compound **3** has been described in a previous study[30]. Here, we describe the synthesis of the compounds **1** and **2**, according to Scheme 1, using the *cis-* $[RuCl_2(dppb)(bipy)]$[31] as a precursor. The molar conductivity measurements of compounds **1** and **2** were performed in CH_2Cl_2, and the results [42.5 μS/cm for **1** and

41.4 µS/cm for **2**] indicated that they are electrolytes 1:1 (CH_2Cl_2 range 1:1 = 12-77

µS/cm)[56]. The cyclic voltammetric experiments for the compounds **1** and **2,** carried out

in CH_2Cl_2 solutions, presented a *quasi*-reversible process, corresponding to a one-

electron Ru^{II}/Ru^{III}, with $E_{1/2}(E_{pa} + E_{pc}/2)$ values close to 868 mV for **1**, 1012 mV for **2**

and 1016 mV for **3** against the reference Ag/AgCl electrode.

<div align="center">**Insert scheme 1**</div>

As can be seen in scheme 1, the compounds **1** and **2** contain three chelated

ligands, and differ from precursor by absence of two chlorides and the charge. The

reaction was followed by the $^{31}P\{^1H\}$ NMR experiments. The precursor

[$RuCl_2$(bipy)dppb)] spectrum presents a pair of doublets (43.0 and 32.0, ppm with $^2J_{P-P}$

= 32.0 Hz)[31, 57], meanwhile the $^{31}P\{^1H\}$ NMR spectra of **1** and **2** present the pair of

doublets at 42.00 (d); 41.24 (d), and 42.83 (d); 40.46 (d) ppm, with $^2J_{P-P}$ = 35.64 Hz and

36.45 Hz, respectively, indicating the coordination of the N–S chelating ligand, which is

confirmed by single-crystal X-ray experiments (Figure 1). The data collections and

experimental details are summarized in Table 1. Selected bond lengths and angles are

presented in Figure 1 caption. The PF_6^- counter-ion is disordered, and disordered in two

positions in both structures. For clarify, it was not included in the figures of the

compounds.

<div align="center">**Insert Figure 1**</div>

The phosphorus atoms are disposed *trans* to the nitrogen atoms, one from the

bipy ligand and the other from the Spy⁻ and Spym⁻ ligands. The sulfur atom is

positioned *trans* to the remaining bipy nitrogen atom. The Ru-P distances for **1** and **2** are within the normal range found for Ru(II) tertiary phosphine compounds[30, 58, 59]. The P–Ru–P angles for the seven-membered ring of dppb in **1** and **2** are 94.44(7) Å and 94.56(4) Å, which are comparable to the values previously observed in the literature for other Ru–dppb compounds[30, 31, 60, 61].

The Ru–S distances of 2.42(12) Å for **1** and 2.41(19) for **2** are practically identical to those observed for **3** and other similar compounds containing thiolate ligands[30, 62]. The C–S bond distance of 1.74(5) Å for **1** and 1.73(8) Å for **2** are significantly longer than the expected C-S double-bond distance of 1.62 Å, but shorter than the C–S single-bond distance of 1.81 Å, as can be observed for **3**[30].

Compounds **1** and **2** are isostructural, they present almost identical cell parameters, same Pbca space group and crystal self-assembly containing eight molecules per cell. The molecular difference between them is only to change one N atom in the structure of the Spym ligand, by CH in the Spy. On the other hand, the complex **3** crystalizes in the $P2_1/n$ space group with four molecules per unit cell and molecular arrangement different than that one adopted by **1** and **2**. This aspect is an influence of the presence of two methyl groups as substituents in the $SpymMe_2$ ligand that increase the steric hindrances.

The stability of the compounds were supported by $^{31}P\{^1H\}$ NMR and molar conductance experiments in which DMSO solutions of **1-3** were left to stand for 10 days at room temperature. No changes were observed on spectral and conductivity values (data not shown).

Insert Table 1

3.2.Anti-proliferative activity of compounds 1-3, *in vitro*

The anti-proliferative activities of the three compounds were assessed by MTT assay, monitoring their capacities to inhibit HepG$_2$, MDA-MB-231 and CHO cell growth. HepG$_2$ cells are characterized by enhanced xenobiotic metabolizing capacity, inducing the activity of enzymes, which play a fundamental role in the activation and detoxification of pro-carcinogen genotoxins[63]. The compounds were also tested on non-tumoral CHO cells.

MDA-MB-231, HepG$_2$ and CHO cells were exposed to the ruthenium compounds in different concentrations or to the vehicle, as mentioned in the experimental section, for a period of 24 h. In another set of experiments, the cells were exposed to doxorubicin and cisplatin as a positive control. The IC$_{50}$ values, calculated from the dose-survival curves generated by the MTT assay are shown in Table 2.

The results gave that the anti-proliferative activity of compounds **1-3** is 5 to 7 times higher than cisplatin and 1.4 to 2.2 times higher than doxorubicin against HepG$_2$ cancer cells; 80 to 134 times higher than cisplatin and 1.8 to 3.1 times higher than doxorubicin against MDA-MB-231. These findings encouraged us to study the mechanism of action of **1-3**, evaluating their interaction with different systems.

Insert Table 2

3.3.Ct-DNA binding experiments

3.3.1. Compound-DNA interactions by UV-Visible titrations

All compounds exhibit the same behavior when ctDNA is added; in which absorption spectra decrease at the ratio of about 5.8 - 7.1 %, suggesting a weak interaction between compounds and DNA. The binding constant Kb of the compounds

with ctDNA, can be calculated by the slope of the straight line obtained from equation 1[64]:

$$[DNA]/ (\varepsilon_a-\varepsilon_f)= [DNA]/(\varepsilon_b-\varepsilon_f) + 1/ Kb(\varepsilon_b-\varepsilon_f) \text{ (Equation 1)}$$

in which [ctDNA] is the concentration of ctDNA in base pairs, ε_a is the ratio of the absorbance/[Ru] , ε_f is the extinction coefficient of the free Ru(II) compound, and ε_o is the extinction coefficient of the compound in the fully bound form. The ratio of the slope to the intercept in the plot of $[DNA]/(\varepsilon_a-\varepsilon_f)$ vs. [DNA] gives the value of Kb, which was calculated absorption band (λmax) at around 300 nm. Figure 2 depicts electronic spectra obtained for compound **3**, which is similar to those obtained for compounds **1** and **2**. Kb values of about $10^4 \, M^{-1}$, showed on Table 3 for compounds **1–3,** are comparable with those found for *trans*-[Ru(PPh$_3$)$_2$(BzPh$_2$Th)(bipy)]PF$_6$ and *trans*-[Ru(PPh$_3$)$_2$(FuPh$_2$Th)(bipy)]PF$_6$ and other cationic Ru(II) compounds that bind to DNA through electrostatic[65]. This suggests that considering the molecular structure and positive charge of the compounds, electrostatic interactions with ctDNA are expected, involving the negatively charged phosphate groups of DNA. In addition, Kb values of compounds **1-3** are lower than those observed for the classical intercalator ethidium bromide (Kb $\geq 10^6 \, M^{-1}$)[66].

Insert Figure 2

Insert Table 3

3.3.2. Compound-DNA interactions performed by square-wave voltammetry (SWV)

Investigation of the interaction of the three compounds with the DNA through SWV indicates a shifts of the redox potential toward negative values, with a Δ of 23 for **1**, 33 for **2** and 36 mV for **3** (Figure 3), indicative of an electrostatic compound-DNA interaction[67], probably through the phosphate group of the DNA backbone. Comparison of the Kb values obtained through of UV-Visible and SWV techniques indicate that the two parameters are in correlation with the largest Kb values, corresponding to the largest Δ values.

Insert Figure 3

3.3.3. Compound-DNA interactions performed by viscosity

The effect of the compounds on the perturbation of the DNA relative viscosity (η/η_0) is reported in Figure 4. No significant change are observed by changing the concentration of the compound, indicating that the compounds do not intercalate to the DNA and indicating that the compound-DNA interaction has mainly an electrostatic character[31], as also suggested by the square wave voltammetry measurements.

Insert Figure 4

3.4. BSA Interactions study

Bovine Serum Albumin (BSA) is used as a model protein in biomimetic systems, since it is the most abundant protein in bovine blood (typically a concentration of 50 mg mL^{-1}) and presents a very similar structure to Human Serum Albumin (HSA)

which shows 76% of identical amino acid sequence homology[68]. The interaction of

complex-BSA has been studied following the BSA fluorescence quenching process

using the equation 2 of Stern-Volmer:

$$F_0/F = 1 + K_{sv}[Q] = 1 + K_q t_0[Q] \text{ (Equation 2)}$$

where F_0 is the fluorescence intensity in the absence of the compound; F is the

fluorescence intensity, in the presence of the compound; [Q] is the concentration of the

compound and K_{sv} is the Stern-Volmer constant; K_q is the bimolecular rate constant

suppression; t_0 is the average lifetime of fluorescence of BSA without the compound[69].

The constant K_{sv} obtained plotting F_0/F versus [Q], and K_q is obtained as the ratio

between t_0 (6.2×10^{-9} s) and K_{sv}.

The fluorescence quenching has been studied at different temperature to

discriminate between static and dynamic quenching[28]. As can be seen in Figure 5, the

Stern–Volmer constants do not change significantly when the temperature is increased,

indicating that fluorescence quenching does not occur through a dynamic collision, but

through the formation of an intermediate species [70].

Fluorescence quenching can be used to evaluate the binding constant K_b between

the compound and BSA, using the equation 3[34]:

$$Log(F_0-F)/F = \log K_b + n \log[Q] \text{ (Equation 3)}$$

where K_b is the binding constant between the compound and BSA, and n is the number

of binding sites per BSA molecule. The constant K_b is obtained from the linear

coefficient of the straight line obtained by the graph of log $[(F_0-F) / F]$ *versus* log [Q]. The number of binding sites (n) can be calculated from the slope of equation(3)[71]. The plot of K_b against 1/T permits to evaluate the enthalpic and entropic contribution to the binding of complex-BSA, using the equation 4 [28]:

$$lnK_b= -(\Delta H^o/RT)+(\Delta S^o/R) \text{ (Equation 4)}$$

The results are shown in Figure 5.

Insert Figure 5

The Kb for the compounds **1-3,** with BSA ranges between 10^4-10^5 and the results showed that the compounds bind to single specific site, since the n value is approximately 1 (Table 4).

Insert Table 4

The interaction between the compounds and BSA has mainly a hydrophobic character and it characterized by an intermediate ΔG value since both the enthalpic and entropic terms are positive and it is likely that it occurs in the proximity of Trp-212. The magnitude of the BSA-binding constant of **1** - **3**, compared with other Ru(II) compounds reported recently [72], suggests a moderate interaction with BSA molecule.

Evaluation of mutagenic activity

3.4.1. Ames Test

The mutagenicity of the compounds **1-3** was assessed by the Ames test[35], using five different compound concentrations and four bacterial strains (*Salmonella typhimurium* TA97a, TA98, TA100 and TA102), each strain carrying different mutations in various genes in the histidine operon, according to the international guidelines[34]. A metabolic activation system (S9 mix) was added to *S. typhimurium* during the assay to metabolize the compounds by cytocrome P450.

Table 5 shows the mean number of revertants/plate (M), the standard deviation (SD) and the mutagenic index (MI) after the treatments with the three ruthenium compounds, observed in *S. typhimurium* strains TA98, TA100, TA102 and TA97a, in the presence (+S9) and absence (−S9) of metabolic activation. The mutagenicity assays showed that the compounds do not induce any increase in the number of the revertant colonies, relative to the negative control, and the mutagenic index (MI) is not higher than 2 at any tested concentration, indicating the absence of mutagenic activity.

3.4.2. Cytokinesis-blocked micronucleus cytomeassay(CBMN-cyt) in HepG2 cells

The chromosome damage induced by the ruthenium compounds was assessed by evaluating the frequencies of micronucleus (MN), nucleoplasmatic bridges (NPBs) and nuclear buds (NBUDs) in binucleated HepG2 cells. The positive control (doxorubicin) caused a significant increase in MN frequencies compared to the control group, in which HepG2 cells were treated for 24 h with the vehicle. Frequencies of MN binucleated cells following HepG2 cell treatment with **1-3** did not increase MN frequencies (data not shown). The results clearly demonstrated that compounds do not induce chromosome damage on HepG2 cells on assayed concentrations.

24

Chemical and physical agents may act as initiators of genetic irreversible alterations leading to the origin of heterozygous cells for oncogenic mutations[73]. Chemotherapeutic agents, such as cisplatin and cytosine arabinoside, may promote carcinogenesis in pre-malignant cells and lead to the development of second malignances through the induction of mitotic recombination. Actually, numerous reports have been associated with the effects of chemotherapeutic agents and the pathogenesis of second malignant neoplasms[74, 75]. It is almost axiomatic that DNA-binding agents are mutagens and frameshift mutagenicity is a characteristic of many intercalators. Indeed, this property is likely to be a major factor in the carcinogenicity of such agents and is an adverse property that should be eliminated by rational drug design, when possible[76]. Thus, the lack of mutagenic activity for the three here presented ruthenium compounds, evaluated through the Ames test and CBMN-cyt encourage further studies about their possible use as anticancer agents.

Insert Table 5

3.5. Topoisomerase IB activity

The effect of **1-3** in the inhibition of the relaxation activity of topoisomerase IB was assessed by a plasmid relaxation assay, incubating a supercoiled plasmid with the enzyme in the absence or presence of different compound concentrations (Figure 6. A, B and C). The relaxation activity monitored at 10 min after incubation indicates that the compounds inhibit Top 1 activity in a dose dependent manner, and **3** is the most active compound, since a full Top1 inhibition is achieved at 25 µM (Figure. 6C, lane 9), while for **2** a full inhibition occurs at 50 µM (Figure. 6B, lane 10). For **1** a full inhibition was not reached, even at a very high concentration of the compound (Figure. 6A). The band

of the supercoiled plasmid, in the absence of enzyme, has an identical height in the absence and in presence of a large compound concentration indicating that none of the three compounds interact with the DNA substrate at this concentration (Figure. 6 A, B and C, lane 2). We suggest that the higher molecular volume of the compound **3**, presenting two methyl groups in the SpymMe$_2$ ligand can contribute to the inhibition capacity of **3** compared to **1** and **2**, by directly binding to Top1 or Top 1-DNA complex.

A lower concentration of **3** is sufficient to have a complete inhibition of topoisomerase IB activity, when the compound is pre-incubated with the enzyme. In detail, a concentration of 6.25μM of compound **3** fully inhibits the enzyme when pre-incubated for 5 min before adding the DNA substrate, suggesting that the compound directly interacts with the enzyme (Figure. 7, lane 14–16).

The compounds **1-3** show antitumor activity with very similar IC$_{50}$ values, on the other hand, **3** is the most potent Top I inhibitor. In a structure-activity study of camptothecin derivates, Jaxel et al. (1989)[77] concluded that the perfect agreement between topoisomerase I inhibition and antitumor activity was not obtained and is not to be expected, because drug metabolism and barriers to cell penetration may in some cases markedly alter biological effectiveness. This fact can explain the similar IC$_{50}$ values for three compounds in several cells lines and differences on Top 1 inhibitory capacity when compounds are evaluated interacting directly with Top1.

3.6.Analysis of cleavage and religation kinetics

The cleavage and relegation reactions were performed in separate experiments to clarify if the compound **3**, the most potent Top 1 inhibitor, affects one or both steps of the catalytic cycle. The cleavage kinetics were studied reacting Top1 with the suicide substrate (Figure. 8A), in the absence and in the presence of the compounds. Analysis of

the reaction products are shown in Figure 8B and 8C. The cleavage kinetics is fast in the

absence of the compound, whilst it is completely inhibited in the presence of 50μM of

compound **3** (Figure 8B) or 6.25μM of compound **3** pre-incubated with Top1, before

substrate addition (Figure 8C).

The religation kinetics were carried out incubating the suicide cleavage substrate

with Top1 for 30 min, to produce the cleaved complex, followed by a subsequent

addition of 200-fold molar excess of the R11 complementary oligonucleotide (Figure 9.

A) in the presence of DMSO or compound **3**. The data show that the religation kinetics

of Top1 (Figure 9. B, lane 2–8) is slowed down in the presence of 50 μM of **3** (Figure 9.

B, lane 9–15).The effect is more evident in the first minutes of the mixture. In the

absence of compound **3,** the band of the religated product is already observed at 0.5

minute, whilst in its presence, a band of similar intensity is observed after 1 minute

(Figure 9, B).

3.7.Topoisomerase IB–DNA interaction study

The ability of compound **3** to affect the enzyme–DNA binding was monitored

through a DNA electrophoretic mobility shift assay, carried out with the inactive Y723F

mutant. The shifted band, corresponding to the DNA–Top1 complex, is only observed

when the substrate is incubated with the enzyme, but not in the presence of 50 μM of

compound **3** (Figure 10). This result indicates that the cleavage step is inhibited because

the compound does not permit the binding of the enzyme to DNA, thus explaining the

inhibition of the cleavage reaction reported in Figure 8. Indeed, the ability of the

compound **3** to interact with Top1, hinders the DNA-Top1 complex formation.

Insert Figure 6

Insert Figure 7

Insert Figure 8

Insert Figure 9

Insert Figure 10

3.8.Prediction of the compound 3 binding mode by molecular docking

The interaction of compound **3** either with the free protein or with the Top 1-DNA complex was analyzed by molecular docking, which was initially performed with the free protein, since the compound inhibits the DNA binding to the protein, as observed by the EMSA assay (Figure 11). The 250 docked structures, characterized by a relatively large spread, can be clustered in 3 main families (Figure 11 A), with binding energies ranging between -6.2 and -5.3 Kcal/mol. The two most populated families are located in the proximity of the active site and the linker domain (Figure 11). They are in contact with Arg634, known to be important for the interaction of the protein with DNA[78], located near His632 belonging to the catalytic pentad. In this position the compound **3** interferes with the DNA binding, providing an explaining for the experimental results.

Docking was also carried out using covalent protein-DNA cleavage complex as a receptor, in order to study at molecular level, the inhibition of the religation step (Figure 11 B). The docking gives rise to 250 docked structures, than can be grouped in 41 clusters, among which 23 belong to 3 main families with a binding energy ranging between -9.41 and 5.9 Kcal/mol. In the most populated family, compound **3** lays on the

DNA groove downstream the cleavage site stabilized by a small number of interactions with the enzyme (Figure 11B). The ruthenium compound, due to its octahedral geometry is not able to intercalate the DNA at the cleavage site as CPT does, but it lays on the DNA groove downstream the cleavage site, likely partially inhibiting the religation due to steric hindrance that constraints the DNA structure.

Recently, Katkar et al. (2014)[21] reported Top 1 inhibition for Cu and Zn compounds. In this study Cu compound is about 6-fold more efficient to inhibit Top 1 activity than Zn one. The authors attribute the efficiency of Cu compound due to its spare planar geometry that allow a direct coordination of the metal with two amino acids (Glu492, Asp563) of the enzyme, differently the tetrahedral Zn geometry only permits a loose interaction with Top 1, explaining the need for larger zinc compound concentrations in order to inhibit similarly the cleavage and the relaxation reaction. The compound **3** evaluated in the present manuscript is 2 times more active than those Cu one and 12 times more active than Zn one compounds. These data show that Top1 inhibition efficiency of compounds are not related to geometry, since molecular docking show that the Ru-based compounds which have octahedral geometry binds close to the residues of the Top 1 active site when enzyme is free, fulfilling the active site better, inhibiting the binding of enzyme to DNA and consequently the cleavage reaction. Moreover **3** can stabilize the Top1-DNA complex and slow down the religation reaction.

Insert Figure 11

4. Conclusion

We presented the synthesis and characterization by spectroscopy, cyclic voltammetry and X-ray crystallography of two new ruthenium compounds [Ru(pySH)(bipy)(dppb)]PF$_6$ (**1**), [Ru(HSpym)(bipy)(dppb)]PF$_6$ (**2**) and compared their biological activities with the analog [Ru(SpymMe$_2$)(bipy)(dppb)]PF$_6$ (**3**), a potent agent against breast tumor cell. Our findings show antiproliferative activity of **1-3** against HepG2 cell line, 5 to 7 times higher than the metallodrug cisplatin (Table 2). Compound/BSA binding studies indicate a spontaneous interaction between these two species and the presence of hydrophobic forces between them. Compound/DNA interaction studies carried out show that **1-3** can bind to DNA through electrostatic interactions.

All the compounds do not display mutagenic activity as evaluated by CBMN-Cyt and Ames test in presence or absence of metabolic activation with S9 from liver rat. Since chemotherapeutic agents, such as cisplatin, may promote carcinogenesis in pre-malignant cells through its mutagenic capacity, the lack of mutagenicity of **1-3** encourage further studies about their possible use as anticancer agents.

One possible target of this class of compounds is human topoisomerase I, since compounds **1-3** inhibit the DNA relaxation by Top1 in a dose dependent (Fig.6). Compound **3,** is the most efficient one and when it is pre-incubated with the enzyme, displays an enhanced inhibitory capacity, suggesting that it directly interacts with the enzyme (Fig. 7). In presence of compound **3**, Top1 is not able to bind the DNA substrate as shown by a shift assay analysis (Fig. 10). Molecular docking indicates that compound **3** preferentially binds close to the residues of the Top 1 active site, when enzyme is free, likely impeding the DNA substrate binding and also explaining the full inhibition of the cleavage reaction. Moreover compound **3** is able to lays on the DNA

groove downstream the cleavage site, slowing down the religation reaction due to steric

hindrance that constraints the DNA structure. Thus, **3** acts either as an inhibitor or as a

poison and then can be considered as a promising nonmutagenic compound to be better

exploited as a possible anticancer drug.

References

1.   M. Alagesan, N. S. Bhuvanesh and N. Dharmaraj, *Dalton Trans.*, 2013, **42**,

        7210-7223.

2.   E. Espinosa and C. G. Raposo, in *Macromolecular Anticancer Therapeutics*,

        Springer, 2010, pp. 3-35.

3.   C. S. Menezes, L. C. de Paula Costa, V. de Melo Rodrigues Avila, M. J.

        Ferreira, C. U. Vieira, L. A. Pavanin, M. I. Homsi-Brandeburgo, A. Hamaguchi

        and E. de Paula Silveira-Lacerda, *Chem. Biol. Interact.*, 2007, **167**, 116-124.

4.   E. de Paula Silveira-Lacerda, C. A. S. T. Vilanova-Costa, A. Hamaguchi, L. A.

        Pavanin, L. R. Goulart, M. I. Homsi-Brandenburgo, W. B. dos Santos, A. M.

        Soares and A. Nomizo, *Biol. Trace Elem. Res.*, 2010, **135**, 98-111.

5.   M. Ravera, S. Baracco, C. Cassino, D. Colangelo, G. Bagni, G. Sava and D.

        Osella, *J. Inorg. Biochem.*, 2004, **98**, 984-990.

6.   M. Clarke and M. Stubbs, *Metal Ions Biol. Syst.*, 1995, **32**, 727-780.

7.   M. R. Green, J. E. Woolery and D. Mahadevan, *Expert Opin. Drug Dis.*, 2011, **6**, 291-307.

8.   Y. Liu, A. Kumar, S. Depauw, R. Nhili, M.-H. David-Cordonnier, M. P. Lee, M. A. Ismail, A. A. Farahat, M. Say and S. Chackal-Catoen, *J. Am. Chem. Soc.*, 2011, **133**, 10171-10183.

9.   Y. Pommier, P. Pourquier, Y. Fan and D. Strumberg, *Biochim. Biophys. Acta*, 1998, **1400**, 83-106.

10.   A. Brüning and I. Mylonas, *Arch. Gynecol. Obst.*, 2011, **283**, 1087-1096.

11.   C. M. Raynaud, L. Sabatier, O. Philipot, K. A. Olaussen and J. C. Soria, *Crit Rev. Oncol. Hematol.*, 2008, **66**, 99-117.

12.   R. Narayanan, P. Tiwari, D. Inoa and B. T. Ashok, *Life Sci.*, 2005, **77**, 2312-2323.

13.   K.-J. Du, J.-Q. Wang, J.-F. Kou, G.-Y. Li, L.-L. Wang, H. Chao and L.-N. Ji, *Eur. J. Med. Chem.*, 2011, **46**, 1056-1065.

14.   J. Moukharskaya and C. Verschraegen, *Hematol. Oncol. Clin. North Am.*, 2012, **26**, 507-525.

15.   S. Castelli, O. Vassallo, P. Katkar, C.-M. Che, R. W.-Y. Sun and A. Desideri, *Arch. Biochem. Biophys.*, 2011, **516**, 108-112.

16.   J. C. Wang, *Annu. Rev. Biochem.*, 1996, **65**, 635-692.

17.   J. J. Champoux, *J. Biol. Chem.*, 1981, **256**, 4805-4809.

18.   L. Stewart, M. R. Redinbo, X. Qiu, W. G. Hol and J. J. Champoux, *Science*, 1998, **279**, 1534-1541.

19.   D. A. Koster, V. Croquette, C. Dekker, S. Shuman and N. H. Dekker, *Nature*, 2005, **434**, 671-674.

20.   J. J. Champoux, *Cold Spring Harbor Laboratory Press*, Cold Spring Harbor 1990, **20**, 217-242.

21.   P. Katkar, A. Coletta, S. Castelli, G. L. Sabino, R. A. A. Couto, A. M. da Costa Ferreira and A. Desideri, *Metallomics*, 2014, **6**, 117-125.

22.   J. B. Leppard and J. J. Champoux, *Chromosoma*, 2005, **114**, 75-85.

23.   Y. Pommier, E. Leo, H. Zhang and C. Marchand, *Chem. Biol.*, 2010, **17**, 421-433.

24.   G. Kohlhagen, K. D. Paull, M. Cushman, P. Nagafuji and Y. Pommier, *Mol. Pharmacol.*, 1998, **54**, 50-58.

25.   Y. Pommier, *ACS Chem, Biol.*, 2013, **8**, 82-95.

26.   Y. Pommier, *Chem. Rev.*, 2009, **109**, 2894-2902.

27.   B. Arno, A. Coletta, C. Tesauro, L. Zuccaro, P. Fiorani, S. Lentini, P. Galloni, V. Conte, B. Floris and A. Desideri, *Biosci. Rep.*, 2013, **33**.

28.   C. Tesauro, P. Fiorani, I. D'Annessa, G. Chillemi, G. Turchi and A. Desideri, *Biochem. J.*, 2010, **425**, 531-539.

29.   S. Castelli, P. Katkar, O. Vassallo, M. Falconi, S. Linder and A. Desideri, *Anticancer Agents Med. Chem.*, 2013, **13**, 356-363.

30.   F. B. do Nascimento, G. Von Poelhsitz, F. R. Pavan, D. N. Sato, C. Q. Leite, H. S. Selistre-de-Araújo, J. Ellena, E. E. Castellano, V. M. Deflon and A. A. Batista, *J. Inorg. Biochem.*, 2008, **102**, 1783-1789.

31.   S. L. Queiroz, A. A. Batista, G. Oliva, M. T. do Pi Gambardella, R. H. Santos, K. S. MacFarlane and B. R. James, *Inorg. Chim. Acta*, 1998, **276**, 209-221.

32.   G. Sheldrick, SHELXS 97, *University of Göttingen, Germany*, 1997.

33.   G. Sheldrick, SHELXL 97, *University of Göttingen, Germany*, 1997.

34.   T. Mosmann, *J. Immun. Meth.*, 1983, **65**, 55-63.

35.   P. P. Corbi, A. C. Massabni, A. G. Moreira, F. J. Medrano, M. G. Jasiulionis and C. M. Costa-Neto, *Can. J. Chem.*, 2005, **83**, 104-109.

36.   L. R. Guilherme, A. C. Massabni, A. Cuin, L. A. Oliveira, E. E. Castellano, T. A. Heinrich and C. M. Costa-Neto, *J. Coord. Chem.*, 2009, **62**, 1561-1571.

37.   M. Reichmann, S. Rice, C. Thomas and P. Doty, *J. Am. Chem. Soc.*, 1954, **76**, 3047-3053.

38.   M. T. Carter, M. Rodriguez and A. J. Bard, *J. Am. Chem. Soc.*, 1989, **111**, 8901-8911.

39.   G. Cohen and H. Eisenberg, *Biopolymers*, 1969, **8**, 45-55.

40.   S. Anbu, R. Ravishankaran, A. A. Karande and M. Kandaswamy, *Dalton Trans.*, 2012, **41**, 12970-12983.

41.   P. Živec, F. Perdih, I. Turel, G. Giester and G. Psomas, *J. Inorg. Biochem.*, 2012, **117**, 35-47.

42.   J. R. Lakowicz, Principles of fluorescence spectroscopy, Springer, 3rd Edn, 2006.

43.   D. M. Maron and B. N. Ames, *Mutat. Res.*, 1983, **113**, 173-215.

44.   L. Bernstein, J. Kaldor, J. McCann and M. C. Pike, *Mutat. Res.*, 1982, **97**, 267-281.

45.   F. A. Resende, L. C. Barbosa, D. C. Tavares, M. S. de Camargo, K. C. de Souza Rezende, M. L. E Silva and E. A. Varanda, *BMC Complement. Altern. Med.*, 2012, **12**, 203.

46.   M. Fenech, *Nature Protoc.*, 2007, **2**, 1084-1104.

47.   D. A. Eastmond and J. D. Tucker, *Mutat. Res.*, 1989, **224**, 517-525.

48.   G. Chillemi, P. Fiorani, S. Castelli, A. Bruselles, P. Benedetti and A. Desideri, *Nucleic Acids Res.*, 2005, **33**, 3339-3350.

49.   K. R. Madden and J. J. Champoux, *Cancer Res.*, 1992, **52**, 525-532.

50.   G. M. Morris, R. Huey, W. Lindstrom, M. F. Sanner, R. K. Belew, D. S. Goodsell and A. J. Olson, *J. Comput. Chem.*, 2009, **30**, 2785-2791.

51.   M. R. Redinbo, J. J. Champoux and W. G. Hol, *Biochemistry*, 2000, **39**, 6832-6840.

52.   G. Chillemi, I. D'Annessa, P. Fiorani, C. Losasso, P. Benedetti and A. Desideri, *Nucleic Acids Res.*, 2008, **36**, 5645-5651.

53.   B. L. Staker, K. Hjerrild, M. D. Feese, C. A. Behnke, A. B. Burgin and L. Stewart, *Proc. Natl. Ac. Sci.*, 2002, **99**, 15387-15392.

54.   G. M. Morris, D. S. Goodsell, R. S. Halliday, R. Huey, W. E. Hart, R. K. Belew and A. J. Olson, *J. Comput. Chem.*, 1998, **19**, 1639-1662.

55.   E. Lindahl, B. Hess and D. Van Der Spoel, J. *Mol. Model*, 2001, **7**, 306-317.

56.   R. G. Velho, PhD Thesis, UNIVERSIDADE FEDERAL DE SÃO CARLOS, 2006.

57.   M. O. Santiago, C. L. DONICCI, I. d. S. Moreira, R. M. Carlos, S. L. Queiroz and A. A. Batista, *Polyhedron*, 2003, **22**, 3205-3211.

58.   M. P. de Araujo, E. Valle, J. Ellena, E. E. Castellano, E. N. dos Santos and A. A. Batista, *Polyhedron*, 2004, **23**, 3163-3172.

59.   S. O. Pinheiro, J. R. de Sousa, M. O. Santiago, I. M. Carvalho, A. L. Silva, A. A. Batista, E. E. Castellano, J. Ellena, Í. S. Moreira and I. C. Diógenes, *Inorg. Chim. Acta*, 2006, **359**, 391-400.

60.   G. Von Poelhsitz, M. P. de Araujo, L. A. A. de Oliveira, S. L. Queiroz, J. Ellena, E. E. Castellano, A. G. Ferreira and A. A. Batista, *Polyhedron*, 2002, **21**, 2221-2225.

61.   M. A. Mondelli, A. E. Graminha, R. S. Corrêa, M. M. da Silva, A. P. Carnizello, G. Von Poelhsitz, J. Ellena, V. M. Deflon, G. F. Caramori and M. H. Torre, *Polyhedron*, 2014, **68**, 312-318.

62.   G. Von Poelhsitz, B. Rodrigues and A. Batista, *Acta Crystallogr. Sect. C - Cryst, Struct. Commun.*, 2006, **62**, m424-m427.

63.   L. Burgos, M. Lehmann, D. Simon, H. H. R. de Andrade, B. R. R. de Abreu, D. D. Nabinger, I. Grivicich, V. B. Juliano and R. R. Dihl, *Sci. Total Environ.*, 2014, **490**, 679-685.

64.   A. Wolfe, G. H. Shimer Jr and T. Meehan, *Biochemistry*, 1987, **26**, 6392-6396.

65.   R. S. Correa, K. M. de Oliveira, F. G. Delolo, A. Alvarez, R. Mocelo, A. M. Plutin, M. R. Cominetti, E. E. Castellano and A. A. Batista, *J. Inorg. Biochem.*, 2015.

66.   U. Chaveerach, A. Meenongwa, Y. Trongpanich, C. Soikum and P. Chaveerach, *Polyhedron*, 2010, **29**, 731-738.

67.   M. Sirajuddin, S. Ali and A. Badshah, *J. Photochem. Photobiology B*, 2013, **124**, 1-19.

68.   K. Hirayama, S. Akashi, M. Furuya and K.-i. Fukuhara, *Biochem. Biophys. Res. Commun.*, 1990, **173**, 639-646.

69.   C.-X. Wang, F.-F. Yan, Y.-X. Zhang and L. Ye, *J. Photochem. Photobiol.*, 2007, **192**, 23-28.

70.   M. Ganeshpandian, R. Loganathan, E. Suresh, A. Riyasdeen, M. A. Akbarsha and M. Palaniandavar, *Dalton Trans.*, 2014, **43**, 1203-1219.

71.   S. Tabassum, W. M. Al-Asbahy, M. Afzal and F. Arjmand, *J. Photochem. Photobiol. B*, 2012, **114**, 132-139.

72. M. Alagesan, P. Sathyadevi, P. Krishnamoorthy, N. Bhuvanesh and N. Dharmaraj, *Dalton Trans.*, 2014, **43**, 15829-15840.

73. B. D. Young, S. Debernardi, D. M. Lillington, S. Skoulakis, T. Chaplin, N. J. Foot and M. Raghavan, *Adv. Enzyme Reg.*, 2006, **46**, 90-97.

74. L. Aung, R. G. Gorlick, W. Shi, H. Thaler, N. A. Shorter, J. H. Healey, A. G. Huvos and P. A. Meyers, *Cancer*, 2002, **95**, 1728-1734.

75. R. W. Vancura, J. J. Kepes, K. L. Newell, T. M. Ha and P. M. Arnold, *Surg. Neurol.*, 2006, **65**, 490-494.

76. S. Venitt, C. Crofton-Sleigh, M. Agbandje, T. C. Jenkins and S. Neidle, *J. Med. Chem.*, 1998, **41**, 3748-3752.

77. C. Jaxel, K. W. Kohn, M. C. Wani, M. E. Wall and Y. Pommier, *Cancer Res.*, 1989, **49**, 1465-1469.

78. I. D'Annessa, C. Tesauro, Z. Wang, B. Arnò, L. Zuccaro, P. Fiorani and A. Desideri, *BBA Proteins Proteom.*, 2013, **1834**, 2712-2721.

Graphics
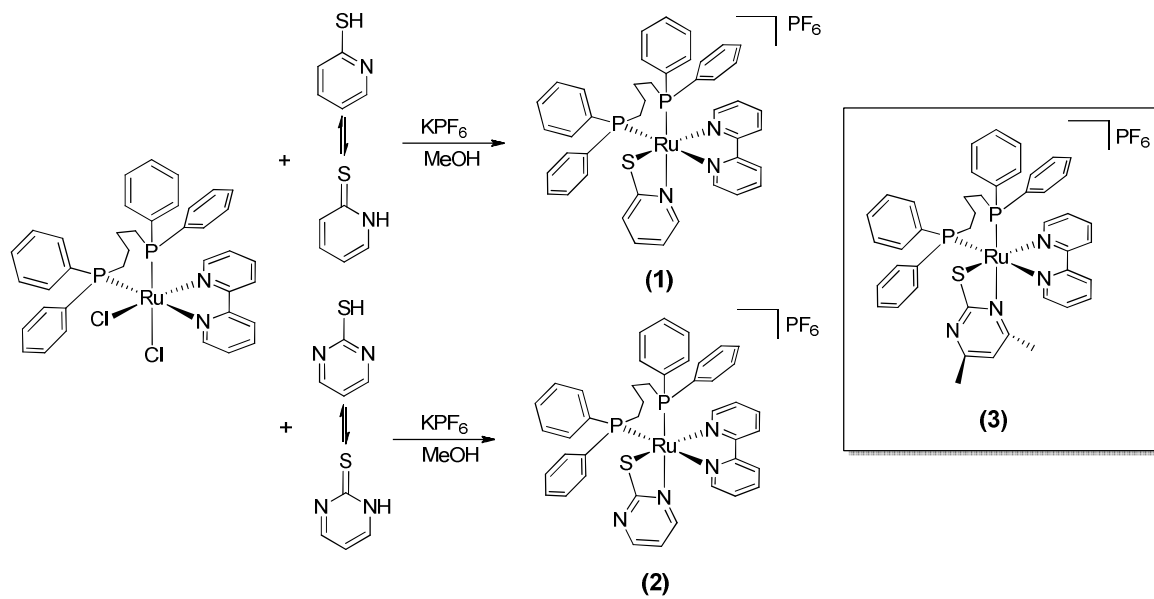
Scheme 1. Synthesis of **1** and **2** and structure of **3**

Compound **1**   Compound **2**
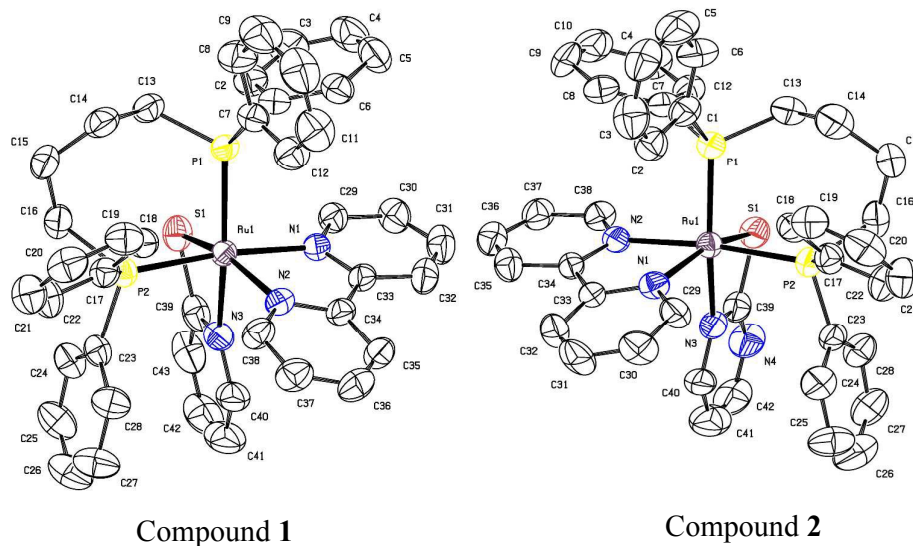
Figure 1. ORTEP of **1** and **2**, with 50% probability, no H atom and no disordered PF_6 are shown. Distances (Å) and angles (^{o}) of **1**: N(1)-Ru(1) 2.137(3), N(2)-Ru(1), 2.118(3) N(3)-Ru(1) 2.127(3), P(1)-Ru(1) 2.3128(11), P(2)-Ru(1) 2.3356(11), S(1)-Ru(1) 2.4181(12), C(39)-S(1) 1.737(5), N(1)-Ru(1)-N(3) 90.8(2), N(1)-Ru(1)-N(2) 77.4(2), N(3)-Ru(1)-N(2) 83.8(2), N(1)-Ru(1)-P(1) 107.57(16), N(3)-Ru(1)-P(1) 159.79(17), N(2)-Ru(1)-P(1) 91.87(15), N(1)-Ru(1)-P(2) 99.52(17), N(3)-Ru(1)-P(2) 90.59(16), N(2)-Ru(1)-P(2) 173.58(15), P(1)-Ru(1)-P(2) 94.44(7), N(1)-Ru(1)-S(1) 156.76(17), N(3)-Ru(1)-S(1) 67.62(17), N(2)-Ru(1)-S(1) 91.16(15), P(1)-Ru(1)-S(1) 92.81(7), P(2)-Ru(1)-S(1)89.66(7). Distances (Å) and angles (^{o}) of **2**: N(1)-Ru(1) 2.119(6), N(2)-Ru(1) 2.139(5), N(3)-Ru(1) 2.124(6), P(1)-Ru(1) 2.3115(19), P(2)-Ru(1) 2.3353(19), S(1)-Ru(1) 2.4066(19), C(39)-S(1) 1.725(8), C(40)-N(3) 1.341(9), N(2)-Ru(1)-N(3) 90.40(14), N(2)-Ru(1)-N(1)77.35(13), N(3)-Ru(1)-N(1) 83.10(13), N(2)-Ru(1)-P(1) 107.18(10), N(3)-Ru(1)-P(1) 160.26(11), N(1)-Ru(1)-P(1) 91.89(9), N(2)-Ru(1)-P(2) 99.82(10), N(3)-Ru(1)-P(2) 91.10(10), N(1)-Ru(1)-P(2)173.49(9), P(1)-Ru(1)-P(2) 94.56(4), N(2)-Ru(1)-S(1) 156.41(10), N(3)-Ru(1)-S(1) 67.69(11), N(1)-Ru(1)-S(1) 90.89(10), P(1)-Ru(1)-S(1) 93.42(4), P(2)-Ru(1)-S(1) 89.63(4).

2

Table 1. Crystal data refinement of 1 and 2

Compound	1	2
Empirical formula	C43 H40 F6 N3 P3 Ru S	C42 H39 F6 N4 P3 Ru S
Formula weight	938.82	939.81
Temperature	296(2) K	296(2) K
Wavelength	0.71073 Å	0.71073 Å
Crystal system	Orthorhombic	Orthorhombic
Space group	Pbca	Pbca
Unit cell dimensions	$a = 18.6608(13)$ Å; $\alpha = 90°$ $b = 19.9930(15)$ Å; $\beta = 90°$ $c = 21.8841(15)$ Å; $\gamma = 90°$	$a = 18.3794(11)$ Å; $\alpha = 90°$ $b = 19.6522(12)$ Å; $\beta = 90°$ $c = 21.8753(13)$ Å; $\gamma = 90°$
Volume	8164.6(10) Å^3	7901.3(8) Å^3
Z	8	8
Density (calculated)	1.528 Mg/m^3	1.580 Mg/m^3
Absorption coefficient	0.616 mm^{-1}	0.638 mm^{-1}
F(000)	3824	3824
Crystal size	0.19 x 0.13 x 0.10 mm^3	0.11 x 0.06 x 0.05 mm^3
Theta range for data collection	1.76 to 25.06°.	1.78 to 25.08°.
Index ranges	$-22 \leq h \leq 19$, $-23 \leq k \leq 23$, $-26 \leq l \leq 26$	$-21 \leq h \leq 21$, $-23 \leq k \leq 20$, $-26 \leq l \leq 26$
Reflections collected	43260	71846
Independent reflections	7196 [R(int) = 0.0408]	6990 [R(int) = 0.1072]
Completeness to theta = 25.06°	99.5 %	99.7 %
Absorption correction	Semi-empirical fromequivalents	Semi-empiricalfromequivalentes
Max. and min. transmission	0.7452 and 0.7059	0.9688 and 0.9332
Refinement method	Full-matrix least-squares on F^2	Full-matrix least-squares on F^2
Data/ restraints / parameters	7196 / 21 / 512	6990 / 21 / 512
Goodness-of-fit on F^2	1.038	1.025
Final R indices [I>2sigma(I)]	R1 = 0.0445, wR2 = 0.1127	R1 = 0.0661, wR2 = 0.1692
R indices (all data)	R1 = 0.0653, wR2 = 0.1292	R1 = 0.1230, wR2 = 0.2013
Largest diff. peak and hole	0.982 and -0.862 e.Å^{-3}	0.876 and -1.243 e.Å^{-3}
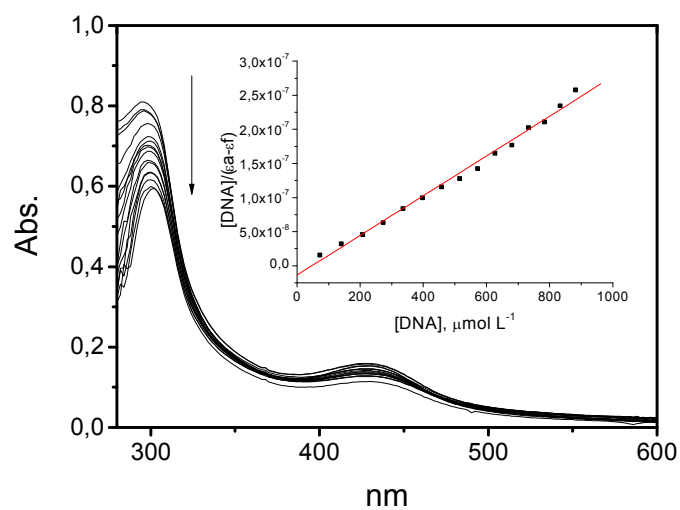
Figure 2: Spectra of compound **3** spectroscopic titration with DNA at concentrations of 7.5×10^{-5} mol L^{-1} and [DNA] = 4.28×10^{-3} mol L^{-1} at pH 7.4.

4

Table 2. Inhibition of cellular viability and calculation of IC_{50} values on $HepG_2$, CHO and MDA-MB-231 cell lines after exposure to compounds **1, 2** e **3**, doxorubicin and cisplatin . The values are the mean ± SEM of three independent experiments carried out in duplicate.

Compounds	IC_{50} (µM) ± SEM		
	$HepG_2$	CHO	MDA-MB-231
1	2.07 ± 0.35	1.97 ± 0.45	0.55 ± 0.41
2	3.23 ± 0.62	3.03 ± 0.52	0.82 ± 0.43
3	2.26 ± 0.37	2.45 ± 0.39	0.49 ± 0.29
Doxorubicin	4.52 ± 0.44	6.03 ± 0.47	1.53 ± 0.62
Cisplatin	16.31 ± 0.74	18.05 ± 0.52	66 ± 4.06

5

1
2
3
4
5
6
7
8
9
10
11
12
13
14
15
16
17
18
19
20
21
22
23
24
25
26
27
28
29
30
31
32
33
34
35
36
37
38
39
40
41
42
43
44
45
46
47
48
49
50
51
52
53
54
55
56
57
58
59
60

Table 3. ct-DNA binding constants (K_b) for the compounds **1-3**

Compound	λ /nm	K_b x 10^4/M^{-1}	hypochromism/%
1	300	1.8 ± 0.2	7.1
2	302	2.0 ± 0.2	5.8
3	300	4.9 ± 0.1	6.3
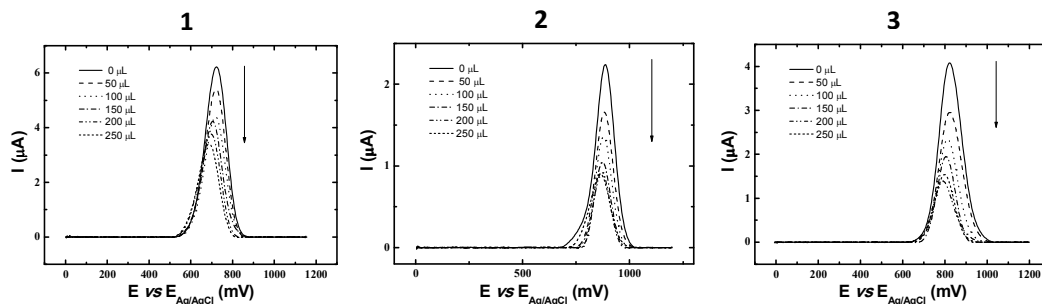
Figure 3. Square-wave voltammograms of 1.0 mM of **1-3** at GC electrode in Tris-HCl buffer (pH 7.4) 30% DMSO as supporting electrolyte, DNA 4.2×10^{-3} molL^{-1}. Frequency = 50 Hz, pulse height = 75 mV and potential increment = 2 mV.
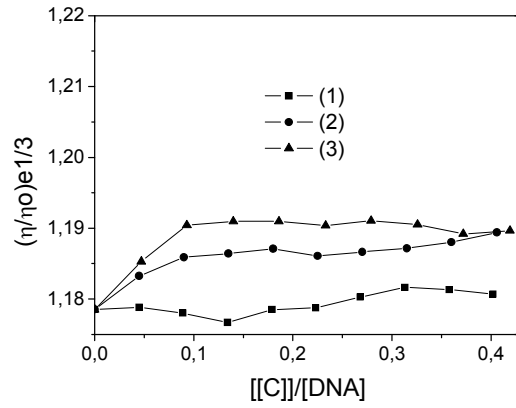
Figure 4: Effect of concentration of compounds related to the viscosity of DNA, at 298 K.
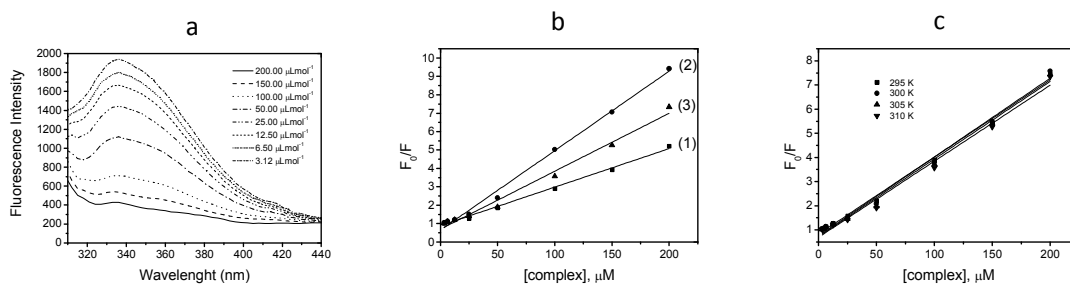
Figure 5. (a) Fluorescence quenching spectra of BSA at different concentrations of **3** at 37°C temperature; excitation wavelength, 295 nm. (b) Plots of relative integrated emission intensity (F_0/F) vs. [compound] for **1–3**. (c) The Stern–Volmer plot for binding the compound with BSA at 295, 300, 305 and 310 K, for **3**.

9

Table 4. BSA-compound interaction and thermodynamic parameters

Compound	T (K)	K_{sv} (10^4 L.mol^{-1})	K_q (10^{12}L.mol^{-1}.s^{-1})	K_b	n	$\Delta H°$ (KJ.mol^{-1}K^{-1})	$\Delta S°$ (J.mol^{-1}K^{-1})	$\Delta G°$ (KJ.mol^{-1})
1	**295**	1.94 ± 0.01	3.13	$(1.72 \pm 0.98) \times 10^4$	0.95			-24.54
	300	2.12 ± 0.02	3.42	$(4.71 \pm 0.27) \times 10^4$	1.06	82.65	363.39	-26.36
	305	2.15 ± 0.02	3.47	$(9.96 \pm 0.65) \times 10^4$	1.14			-28.18
	310	2.16 ± 0.01	3.48	$(8.14 \pm 0.47) \times 10^4$	1.13			-29.99
2	**295**	4.49 ± 0.25	7.24	$(2.18 \pm 0.43) \times 10^5$	1.19			-30.46
	300	5.59 ± 0.24	7.40	$(3.83 \pm 0.89) \times 10^5$	1.25	44.92	255.55	-31.74
	305	4.60 ± 0.20	7.42	$(5.19 \pm 0.11) \times 10^5$	1.29			-33.02
	310	4.51 ± 0.11	7.27	$(5.24 \pm 0.13) \times 10^5$	1.29			-34.30
3	**295**	3.37 ± 0.03	5.44	$(1.01 \pm 0.34) \times 10^5$	1.13			-28.05
	300	3.40 ± 0.07	5.48	$(1.70 \pm 0.29) \times 10^5$	1.19	100.61	436.15	-30.23
	305	3.33 ± 0.04	5.37	$(3.33 \pm 0.81) \times 10^5$	1.27			-32.41
	310	3.22 ± 0.03	5.19	$(7.32 \pm 0.34) \times 10^5$	1.40			-34.59

10

Table 5. Mutagenic activity expressed as the mean and standard deviation of the number of revertants and mutagenic index (MI)(in brackets) in strains TA98, TA100, TA102 and TA97a exposed to compounds 1-3 at various doses, with (+S9) or without (-S9) metabolic activation.

Treatments	Number of revertants (M ± SD)/ plate and MI							
µg/plate	TA 98		TA 100		TA 102		TA 97a	
Compound 1	- S9	+ S9	- S9	+ S9	- S9	+ S9	- S9	+ S9
0,00[a]	27 ± 3	37 ± 4	154 ± 10	161 ± 13	408 ± 17	450± 22	185± 14	203± 9
6.25	30 ± 6 (1.1)	35 ± 2 (0.9)	141 ± 13(0.9)	148 ± 14 (0.9)	377 ± 20 (0.9)	437 ± 16 (0.9)	170 ±21 (0.9)	182 ± 11 (0.9)
12.5	25 ± 3 (0.9)	35 ± 3 (0.9)	138 ± 19(0.9)	152 ± 11 (0.9)	361 ± 18 (0.9)	433 ± 21 (0.9)	191 ± 18 (1.0)	217 ± 20 (1.0)
25	25 ± 4 (0.9)	38 ± 6 (1.0)	153 ± 8(1.0)	145 ± 10 (0.9)	393 ± 28 (0.9)	479 ± 26 (1.0)	176 ± 17 (0.9)	213 ± 19 (1.0)
50	34 ± 3 (1.2)	40 ± 3 (1.1)	160 ± 12 (1.0)	158 ± 17 (1.0)	417± 31 (1.0)	439 ± 39 (1.0)	189 ± 19 (1.0)	237 ± 10 (1.1)
75	29 ± 4 (1.0)	38 ± 5 (1.0)	148 ± 15(0.9)	166 ± 13(1.0)	401 ± 26 (1.0)	480 ± 28 (1.0)	165 ± 13 (0.9)	230 ± 27 (1.1)
C +	1030 ± 57 [b]	1208 ± 103[e]	1321 ± 49[c]	1440 ± 83 [e]	1257 ± 41[d]	1307 ± 32 [e]	1583± 57 [b]	1008±91 [e]
Compound 2								
0,00[a]	21 ± 4	27 ± 4	126 ± 11	144 ± 11	349 ± 21	479± 27	125± 10	122± 11
1.56	17 ± 5 (0.8)	24 ± 7 (0.9)	102 ± 9(0.8)	127 ± 15 (0.9)	355 ± 18 (1.0)	458 ± 19 (0.9)	99 ±18 (0.8)	116 ± 9 (0.9)
3.12	20 ± 5 (0.9)	30 ± 8 (1.1)	100 ± 13(0.8)	147 ± 9 (1.0)	361 ± 15 (1.0)	445 ± 24 (0.9)	101 ± 19 (0.8)	109 ± 15 (0.9)
6.25	19 ± 3 (0.9)	22 ± 5 (0.8)	120 ± 9(0.9)	155± 12 (1.0)	335 ± 29 (0.9)	487 ± 31 (1.0)	112 ± 13 (0.9)	121 ± 6 (1.0)
9.37	22 ± 6 (1.0)	29 ± 5 (1.0)	111 ± 12 (0.9)	159 ± 14 (1.1)	369± 32 (1.0)	458 ± 34 (0.9)	109 ± 17 (0.8)	133 ± 11 (1.0)
12.5	26 ± 3 (1.2)	23 ± 6 (0.8)	128 ± 14(1.0)	164 ± 10(1.1)	359 ± 21 (1.0)	495 ± 27 (1,0)	121 ± 19 (0.9)	129 ± 20 (1.0)
C +	1113 ± 49 [b]	1737 ± 97[e]	2012 ± 48[c]	1853 ± 79 [e]	1163 ± 61[d]	1280 ± 61 [e]	1138± 97 [b]	1112±101 [e]
Compound 3								
0,00[a]	19 ± 5	27 ± 4	77 ± 9	98 ± 9	397 ± 19	403± 23	88± 11	126± 10
1.56	23 ± 5 (0.8)	23 ± 4 (1.1)	80 ± 11(0.9)	85 ± 3 (1.1)	336 ± 18 (1.2)	458 ± 19 (0.9)	80 ±12 (1.1)	115 ± 11 (1.0)
3.12	17 ± 5 (1.1)	27 ± 2 (1.0)	89 ± 12(0.8)	89 ± 4 (0.9)	344 ± 13 (1.1)	438 ± 29 (0.9)	71 ± 17 (1.2)	101 ± 9 (1.2)
6.25	19 ± 4 (1.0)	21 ± 3 (1.2)	79 ± 7(0.9)	98 ± 9 (1.0)	377 ± 15 (1.0)	423 ± 27 (0.9)	70 ± 9 (1.2)	99 ± 12 (1.3)
9.37	18 ± 6 (1.0)	19 ± 1 (1.4)	93 ± 13 (0.8)	103 ± 3 (1.0)	325± 30 (1.2)	415 ± 24 (0.9)	79 ± 13 (1.1)	115 ± 8 (1.0)
12.5	25 ± 4 (0.7)	20 ± 3 (1.3)	88 ± 11(0.9)	100 ± 8(1.0)	357 ± 22 (1.1)	405 ± 17 (1.0)	83 ± 11 (1.0)	106 ± 15 (1.2)
C+	1907 ± 44 [b]	2835 ± 35[e]	1853 ± 56[c]	1900 ± 115 [e]	1392 ± 72[d]	1683 ± 48 [e]	1356± 86 [b]	1765±107 [e]

[a]Negative control: dimethylsulfoxide (DMSO - 100 µL/plate); C+ = Positive control -[b]4 -nitro-o-phenylenediamine (NOPD –10.0 mg/plate – TA98, TA97a); [c]sodiumazide (1.25 mg/plate –TA100); [d]mitomycin (0.5 mg/plate – TA102), in the absence of S9 and [e]2-anthramine (1.25 mg/plate – TA97a, TA98, TA100); [f]2-aminofluorene (10.0 mg/plate – TA102), in the presence of S9.

11
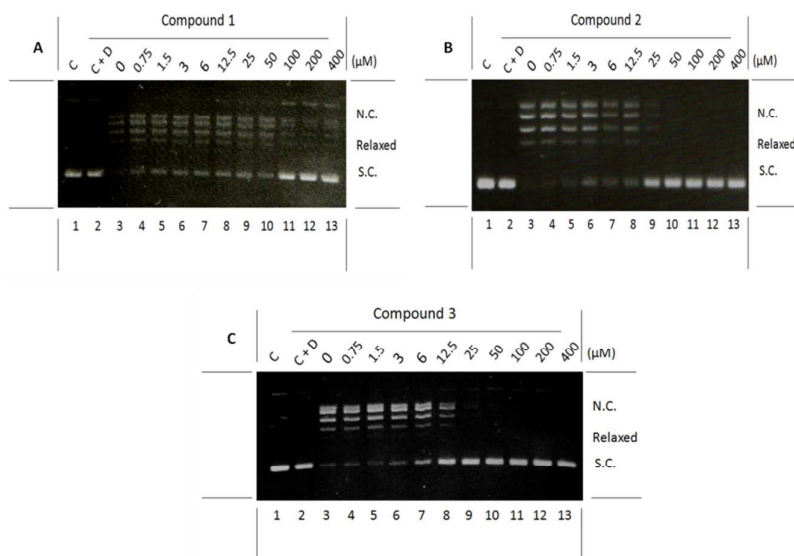
Figure 6. (A, B and C) Relaxation of negative supercoiled plasmid DNA by topoisomerase IB in the presence of increasing concentration of **1**(A), **2**(B) and **3**(C). The reaction products were resolved in an agarose gel and visualized with ethidium bromide. Lane 1, DNA substrate. Lane 2, DNA plus 400 μM of compound. Lane 3, DNA plus enzyme. NC, nicked circular plasmid DNA. SC, supercoiled plasmid DNA.

12
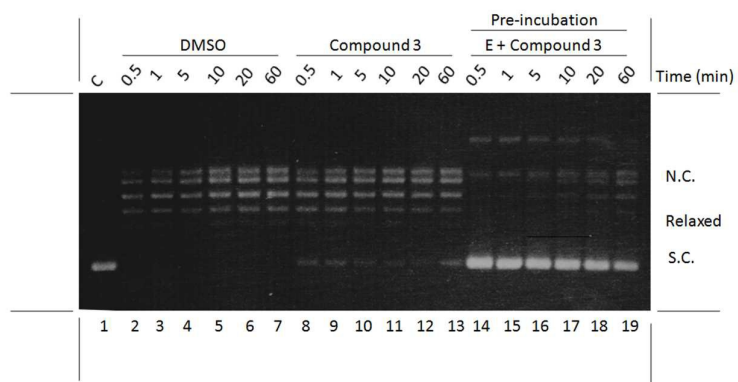
Figure 7. Relaxation of negative supercoiled plasmid DNA in a time course experiment with DMSO (lanes 2–7), in the presence of 6.25 µM of compound **3** (lanes 8–13), after pre-incubation enzyme and 6.25 µM of compound **3** for 5 minutes at 37°C (lanes 14–19). Lane 1, no protein added.
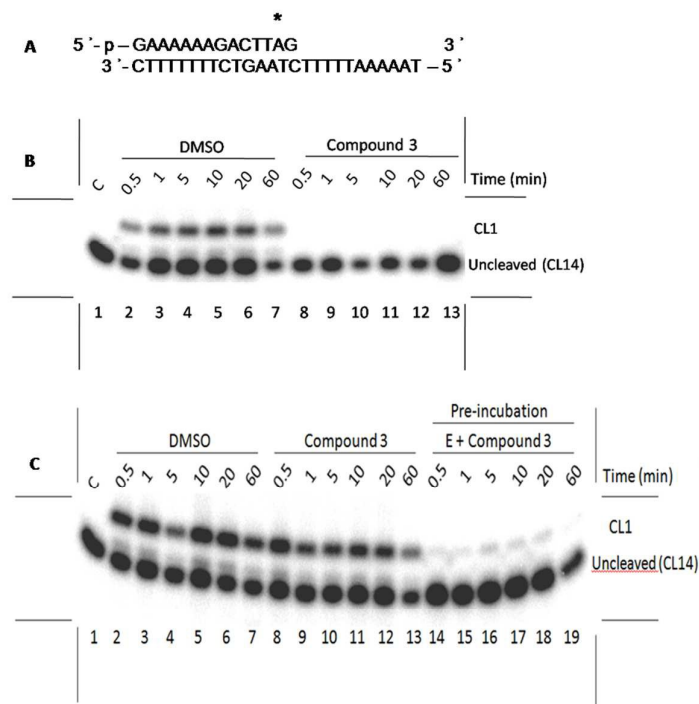
Figure 8. (A) The CL14/CP25 suicide substrate used to measure the cleavage kinetics of the enzyme. The preferred Top1 binding site is indicated by an asterisk. (B) Cleavage kinetics of Top1 in the presence of DMSO (lanes 2–7), in the presence of 50 µM of compound **3** (lanes 8–13). (C) Cleavage kinetics of Top1in the presence of DMSO (lanes 2–7), or 6.25 µM of compound **3** (lanes 8–13), and after 5 min pre-incubation enzyme-compound (lanes 14–19). (B and C), Lane 1 no protein added. CL1 represents the DNA fragment cleaved at the preferred cleavage site.

14
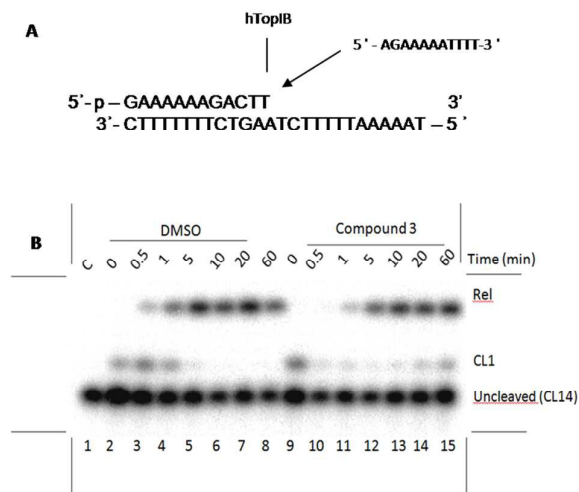
Figure 9. (A) The suicide substrate CL14/CP25 and the R11 complementary oligonucleotide used to measure the religation kinetics of the enzyme. (B) Urea polyacrylamide gel electrophoretic analysis of the religation kinetics of Top1 in the absence (lanes 2–8) or in the presence of 50 µMof compound **3** (lanes 9–15). Lane 1 represents the substrate alone.
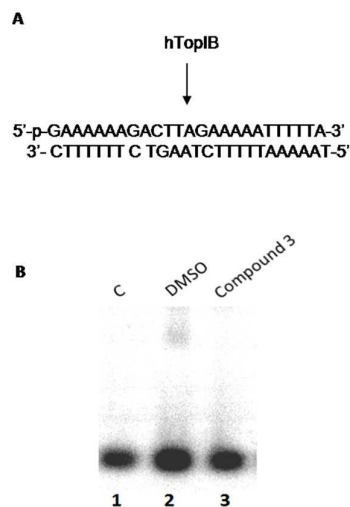
Figure 10. CL25/CP25 substrate (A).Electrophoretic mobility shift assay (B) Lane 1, substrate. Lane 2, DNA in the presence of Y723F Top 1. Lane 3, DNA plus enzyme in the presence of 50 µM of compound **3**.

16
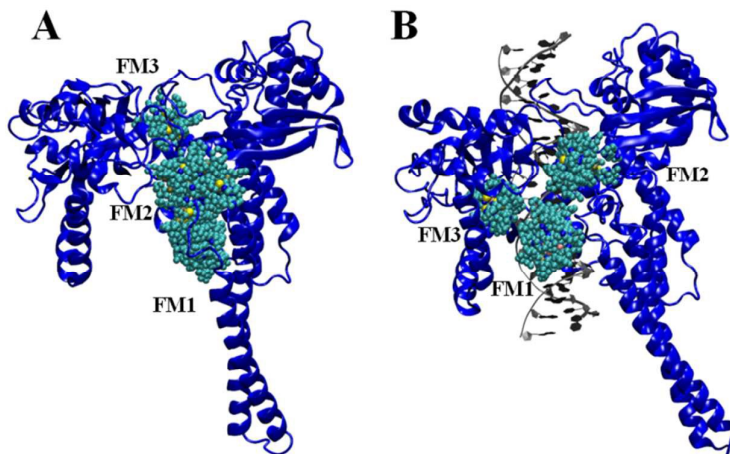
Figure 11. Representation of the three most representative families of the 250 docked structures found upon cluster analysisfor the docking performed with the enzyme free in solution (**A**) and the covalent binary complex (**B**). The acronym FM stands for "family".